2020 Joint International EUROSOI Workshop and International Conference on Ultimate Integration on Silicon (EUROSOI-ULIS) | 978-1-7281-8765-5/20/$31.00 ©2020 IEEE | DOI: 10.1109/EUROSOI-ULIS49407.2020.9365497

Comprehensive Modeling of Coupled Spin and Charge Transport through Magnetic Tunnel Junctions

Simone Fiorentini
CDL for Nonvolatile Memory and Logic
Institute for Microelectronics, TU Wien
Vienna, Austria
fiorentini@iue.tuwien.ac.at

Johannes Ender
CDL for Nonvolatile Memory and Logic
Institute for Microelectronics, TU Wien
Vienna, Austria
ender@iue.tuwien.ac.at

Siegfried Selberherr
Institute for Microelectronics
TU Wien
Vienna, Austria
Selberherr@TUWien.ac.at

Roberto Lacerda de Orio
Institute for Microelectronics
TU Wien
Vienna, Austria
orio@iue.tuwien.ac.at

Wolfgang Goes
Silvaco Europe Ltd.
Cambridge
United Kingdom
wolfgang.goes@silvaco.com

Viktor Sverdlov
CDL for Nonvolatile Memory and Logic
Institute for Microelectronics, TU Wien
Vienna, Austria
sverdlov@iue.tuwien.ac.at

Abstract—**A drift-diffusion approach to coupled spin and charge transport has been commonly applied to determine the spin-transfer torque acting on the magnetization in metallic valves. This approach, however, is not suitable to describe the predominant tunnel transport in magnetic tunnel junctions. Here we demonstrate that by introducing a magnetization dependent resistivity and adjusting the spin diffusion coefficient one can successfully apply the generalized spin and charge drift-diffusion approach also to magnetic tunnel junctions. As a unique set of equations is used for the entire structure, this paves the way to develop an efficient finite element based approach to describe the magnetization dynamics in emerging spin-transfer torque memories.**

Keywords—Spin and charge drift-diffusion, spin-transfer torque, magnetic tunnel junctions, STT-MRAM

I. Introduction

In recent years, the outstanding improvements in the development of computer memories has been possible thanks to the scaling of semiconductor devices. This, however, has increased the stand-by power consumption due to leakages. An efficient way to reduce the power consumption is the introduction of nonvolatility in integrated circuits.

Spin-transfer torque magnetic RAM (STT-MRAM) is an emerging [1-6] nonvolatile memory which possesses a simple structure and is compatible with CMOS technology. In contrast to flash memory, STT-MRAM is fast and has a high endurance. This makes it particularly suitable for stand-alone as well as embedded applications, for example, in Systems-on-Chip, where STT-MRAM is poised to replace SRAM and flash memories.

The binary information in modern magnetic memories is stored as the relative orientation of the magnetization in the magnetic layers of a magnetic tunnel junction (MTJ), cf. Fig.1. When the magnetization vectors are in a parallel state (P), the resistance is lower than in the anti-parallel state (AP). The switching between these two stable configurations can be achieved by an electric current passing through the structure. The electrons passing through the fixed reference layer (RL) become spin-polarized, generating a spin current. When entering the free layer (FL), the spin current acts on the magnetization via the exchange interaction. As the total spin angular momentum must be preserved, if the magnetization in the layers is not aligned, the polarization is quickly absorbed by it, generating the spin-transfer torque [7]. If the current is sufficiently strong, the magnetization of the free layer can be switched between the two stable configurations, parallel or anti-parallel, relative to the reference layer.

Modeling of STT switching can be performed by assuming a Slonczewski-like torque approach [8]. This, however, allows to approximately simulate the magnetization dynamics of the free layer only. A more complete description of the process can be obtained by computing the non-equilibrium spin accumulation across the whole structure. This task is performed by solving the spin and charge drift-diffusion equations in a *spin valve*, where two ferromagnetic layers are separated by a *metal* [9], [10]. Modern STT-MRAM cells, however, use a magnetic tunnel junction for the memory bit. In this work, we propose a method to solve spin and charge drift-diffusion in this type of structure.

The tunneling resistance defines the current through an MTJ, as it is much larger than the resistances of the ferromagnetic layers. For non-uniform relative

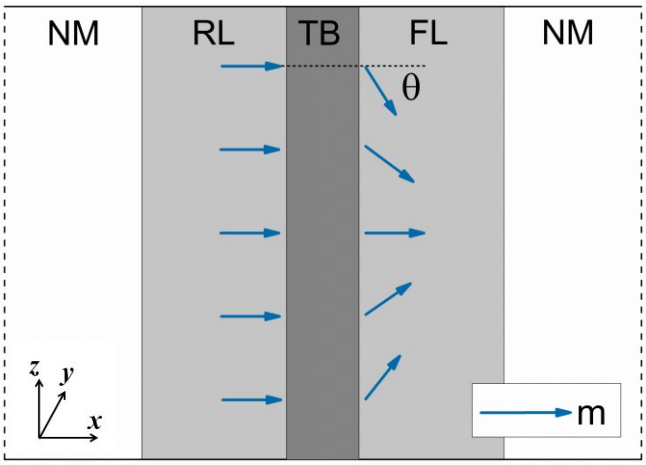

Fig. 1. MTJ structure with non-uniform magnetization configuration. The structure is composed of a reference layer (RL), a tunnel barrier (TB), a free layer (FL), and two non-magnetic contacts (NM).

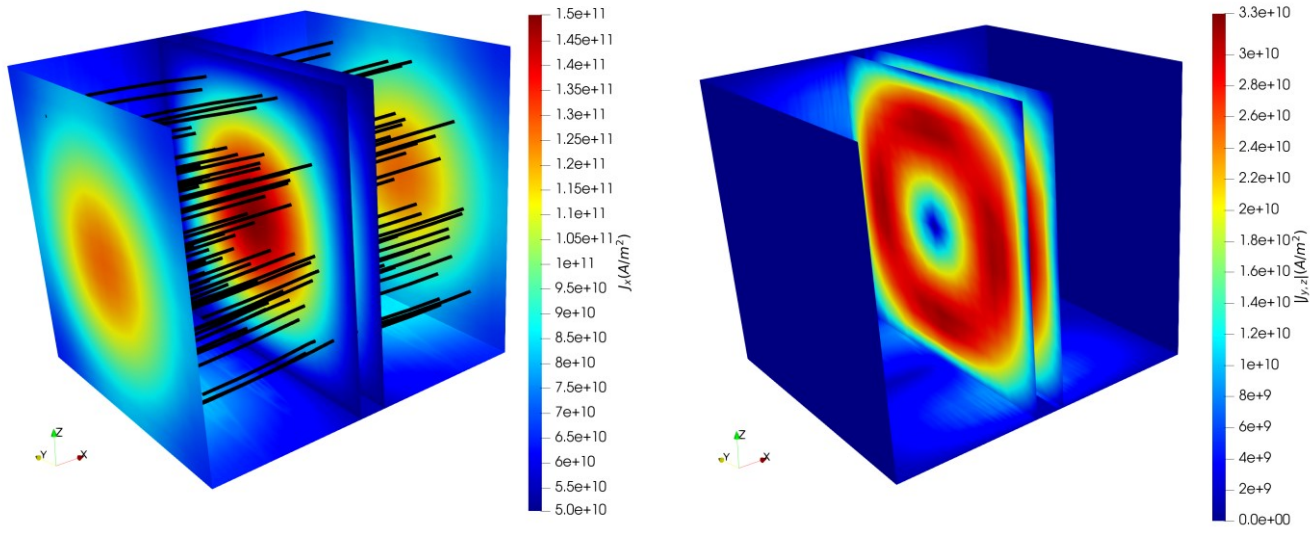

Fig. 2. Current density distribution through a square MTJ with a non-uniform magnetization. The left panel shows the x-component (perpendicular) of the current density, while the right pictures shows the modulus of the y- and z- (in-plane) components. The x-component flow is higher for aligned magnetizations because of the lower resistance. Due to conservation of the current flow, it is redistributed in the yz-plane in the metal contacts (right panel).

magnetization, characteristic to switching, the resistance and the current through an MTJ depend strongly on the position. As Ohm's law must hold, the physical origin resulting in the electrical resistivity is not important. We assume it to be due to charge drift-diffusion in the middle layer. We then model the tunnel barrier as a (poor) conductor whose (large) resistivity depends on the ***relative orientation of the magnetization***. The current can then be used to compute the spin accumulation and extract the torque acting on the magnetization.

II. STT-MRAM

The key element in modern MRAM cells is the MTJ. It is composed of a sandwich of two ferromagnetic layers, usually made of CoFeB, and an oxide layer, usually MgO. The MTJ is characterized by the tunneling magnetoresistance ratio (TMR), defined as

$$TMR = \frac{G_P - G_{AP}}{G_{AP}}, \tag{1}$$

where G_P (G_{AP}) is the conductance in the P (AP) state. A high *TMR* is important to be able to distinguish between the two different configurations. Modern devices can reach a ratio of about 200% and higher [11].

Thin layers of CoFeB on MgO are perpendicularly magnetized, due to the interface-induced perpendicular anisotropy. The switching currents in a perpendicularly magnetized structure are lower than the ones in in-plane magnetized structure, as in this configuration the current-driven and thermally assisted switching go over the same energy barrier. The magnetization vectors of the ferromagnetic layers have two possible stable configurations: parallel and anti-parallel. The magnetization in the so-called free layer is free to switch, while the magnetization in the so-called reference layer is fixed, usually by antiferromagnetic exchange coupling to a pinned layer [12].

Accurate simulation of STT-MRAM demands a solution of the Landau-Lifshitz-Gilbert (LLG) equation describing the magnetization **m** subject to the spin-transfer torque. The equation reads

$$\frac{\partial \mathbf{m}}{\partial t} = -\gamma\mu_0 \mathbf{m}\times\mathbf{H}_{\text{eff}} + \alpha\mathbf{m}\times\frac{\partial \mathbf{m}}{\partial t} + \frac{1}{M_S}\mathbf{T}_\mathbf{S}, \tag{2}$$

where γ is the gyromagnetic ratio, μ_0 is the magnetic permeability, α is the Gilbert damping constant, M_S is the saturation magnetization, and $\mathbf{H}_{\text{eff}}$ includes various contributions, mainly the external field, the exchange interaction, and the demagnetizing field. In order to predict the magnetization behavior during switching, it is necessary to properly compute the STT term, $\mathbf{T}_\mathbf{S}$. This torque is generated by a non-equilibrium spin accumulation **S** acting on the magnetization via the exchange interaction and can be expressed as

$$\mathbf{T}_\mathbf{S} = -\frac{D_e}{\lambda_J^2}\mathbf{m}\times\mathbf{S} - \frac{D_e}{\lambda_\varphi^2}\mathbf{m}\times(\mathbf{m}\times\mathbf{S}), \tag{3}$$

where λ_J, λ_φ, are scattering lengths and D_e is the electron diffusion constant. **S** is created when an electric current passes through the structure and gets polarized by the magnetic layers. In order to obtain **S**, coupled spin and charge transport must be resolved.

When dealing with a spin valve, where the two ferromagnetic layers are separated by a conductive metal layer, it is sufficient to solve the spin and charge drift-diffusion equations in the structure. However, the cell of an STT-MRAM is composed of a *magnetic tunnel junction* (MTJ), a sandwich of two ferromagnets separated by a *tunnel barrier*. It is then necessary to find a way to incorporate the tunnel junction properties when solving the drift-diffusion equations.

III. MTJ MODEL

In an MTJ, the amount of current flowing through the structure is mainly determined by the tunneling resistance, as it is much larger than the resistances of the ferromagnetic layers. As Ohm's law must hold, the high electrical resistivity in the middle layer is assumed to be due to charge drift-diffusion transport. We model the tunnel barrier as a poor conductor whose low conductivity depends on the relative magnetization vectors orientation as

$$\sigma(\theta) = \sigma_0 \left(1+\left(\frac{TMR}{2+TMR}\right)\cos(\theta)\right), \qquad (4)$$

where σ_0 is the average between the conductivities in the P and AP state, and θ is the local angle between the magnetic vectors in the free and reference layer. To obtain the current, we solve the Laplace equation

$$\nabla(\sigma\nabla V) = 0 \qquad (5a)$$

and compute the current with

$$\mathbf{J_C} = \sigma\nabla V, \qquad (5a)$$

where σ is the conductivity, V is the electrical potential and $\mathbf{J_C}$ is the current density. The equation is solved in the structure schematized in Fig.1. The potential is fixed with Dirichlet conditions on the left and right boundaries. The conductivity is constant in the ferromagnetic layers and in the non-magnetic leads, while it is described by (4) in the tunneling layer. For non-uniform relative magnetization, characteristic to switching, the conductivity in an MTJ depends strongly on the position. The solution for the current for this scenario is computed via the finite element method and is reported in Fig.2. The resulting current flowing through the structure is highly non-uniform, with the difference between highest and lowest values of the perpendicular component of the current dictated by the TMR. The absolute values of the in-plane current density are redistributed in order to accommodate for the varying conductivity in the middle layer. Once the current density $\mathbf{J_C}$ is known, the spin current density $\mathbf{J_S}$ and the spin accumulation $\mathbf{S}$ through the barrier are found as [10], [13]

TABLE I. PARAMETERS USED IN THE SIMULATIONS FOR THE MAGNETIC REGIONS

Parameter	Value
β_σ	0.9
β_D	0.8
D_e	$2\text{x}10^{-3}$ m^2/s
λ_{sf}	10 nm
λ_J	2 nm
λ_φ	5 nm

$$\mathbf{J_S} = \frac{\mu_B}{e}\beta_\sigma\left(\mathbf{J_C}+\beta_D D_S\frac{e}{\mu_B}[(\nabla\mathbf{S})\mathbf{m}]\right)\otimes\mathbf{m}-D_S\nabla\mathbf{S} \qquad (6a)$$

$$\frac{\partial\mathbf{S}}{\partial t} = -\nabla\mathbf{J_S}-D_S\left(\frac{\mathbf{S}}{\lambda_{sf}^2}+\frac{\mathbf{S}\times\mathbf{m}}{\lambda_J^2}+\frac{\mathbf{m}\times(\mathbf{S}\times\mathbf{m})}{\lambda_\varphi^2}\right), \qquad (6b)$$

where μ_B is the Bohr magneton, e is the electron charge, β_σ and β_D are polarization parameters, D_S is the spin diffusion constant, λ_{sf} is the spin-flip length, λ_J is the spin exchange length, λ_φ is the spin dephasing length, and $\otimes$ stands for the tensor product.

In order to properly model the properties of a tunnel barrier, it is not sufficient to deal only with the electrical characteristics of the structure. The spin accumulation density must be preserved for electrons tunneling through an ideal barrier without spin flips. To achieve this, one must neglect the spin relaxation by setting all scattering lengths to infinity. However, this is not sufficient. In order to match the spin accumulation through the tunnel barrier within the spin drift-diffusion approach, the ***spin diffusion coefficient*** in the middle region must be set ***large*** compared to the electron diffusion coefficient in the ferromagnetic layers. Fig.3 reports the spin accumulation in the middle layer region. The solution

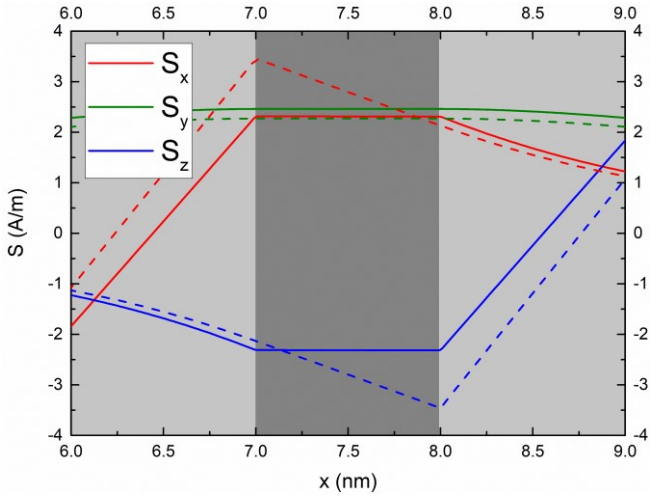

Fig. 3. Spin accumulation across the tunneling layer. The magnetization lies along x in the FL and along z in the RL. The dashed lines are computed using the same value for D_S in TB and D_e in the FL and the RL, while solid lines use a very high value of D_S, which renders $\mathbf{S}$ constant across TB.

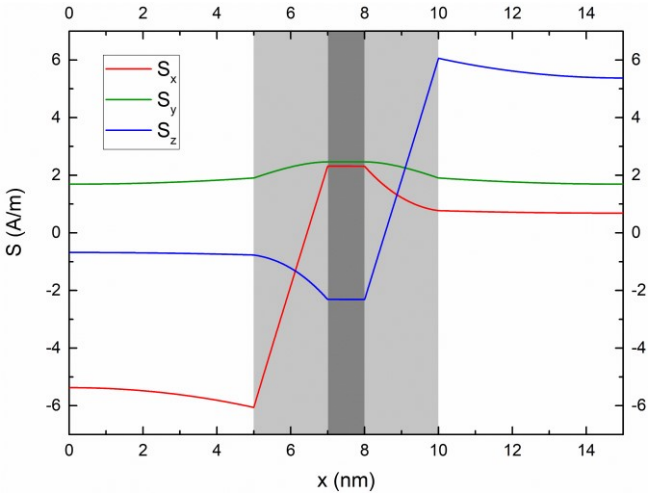

Fig. 4. Spin accumulation solution across the whole structure. The spin accumulation components parallel to the magnetization grow linearly across the ferromagnetic layers, while the perpendicular components decay. The decay is dictated by λ_J and λ_φ.

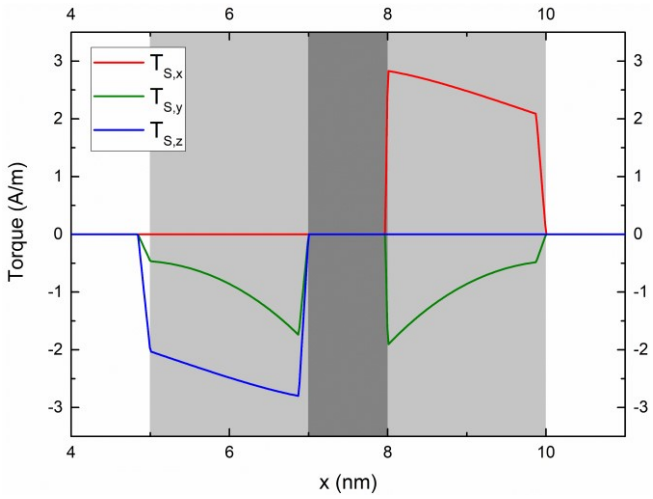

Fig. 5. Torque computed from the spin accumulation. The spin drift-diffusion approach permits to compute the torques acting on both layers, FL and RL.

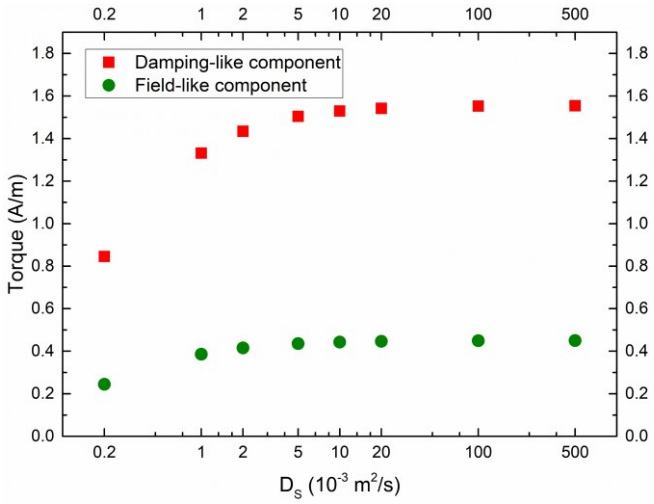

Fig. 6. Magnitude of the torque in the FL as a function of the spin diffusion coefficient in TB. At high values of the coefficient, the torque does not depend on it.

was computed via the finite element approach. The dotted lines represent the solution without the choice of a large spin diffusion coefficient. In this case, the spin accumulation decays through the tunnel barrier. The solid lines represent the solution with a large value for the spin diffusion coefficient. With this choice, the spin accumulation is constant throughout the middle layer. The solution in the whole structure is reported in Fig.4. The non-magnetic leads are necessary, in a multilayer structure, in order to ensure proper boundary conditions. Numerical values for the parameters used in the magnetic regions are reported in Table 1.

With **S** known, we can compute the torques acting on *both* ferromagnetic layers, which are reported in Fig.5. When inserted in the LLG equation, this torque acts on the magnetization and enables switching. We can compute the torque dependence on the value of the spin diffusion coefficient. Results are reported in Fig.6 and show that, provided that the value of the coefficient is large enough, the torque is independent of it.

IV. Conclusion

We presented a method of applying the spin drift-diffusion approach to an MTJ structure. The current can be successfully simulated by modeling the tunnel barrier as a poor conductor with an electrical conductivity locally depending on the relative magnetization orientation in the ferromagnetic layers. In order to properly simulate the spin accumulation, we set all scattering lengths to infinity in the middle layer, and we set the spin diffusion coefficient much larger than the electron diffusion coefficient in the ferromagnetic layers. This way, the spin accumulation can be preserved through the middle layer, as is the case in an ideal tunnel barrier. This generalized spin and charge drift-diffusion approach can be successfully applied to determine the torques acting on the magnetization in a modern STT-MRAM device.

Acknowledgment

The financial support by the Austrian Federal Ministry for Digital and Economic Affairs and the National Foundation for Research, Technology and Development is gratefully acknowledged.

References

[1] S. Aggarwal, H. Almasi, M. DeHerrera, B. Hughes, S. Ikegawa *et al.*, "Demonstration of a reliable 1 Gb standalone spin-transfer torque MRAM for industrial applications," *Proceedings of the IEDM*, pp. 2.1.1-2.1.4, 2019.

[2] K. Lee, J. H. Bak, Y. J. Kim, C. K. Kim, A. Antonyan *et al.*, "1Gbit High Density Embedded STT-MRAM in 28nm FDSOI Technology," *Proceedings of the IEDM*, pp. 2.2.1-2.2.4, 2019.

[3] V. B. Naik, K. Lee, K. Yamane, R. Chao, J. Kwon *et al.*, "Manufacturable 22nm FD-SOI embedded MRAM technology for industrial-grade MCU and IOT applications," *Proceedings of the IEDM*, pp. 2.3.1-2.3.4, 2019.

[4] J. G. Alzate, U. Arslan, P. Bai, J. Brockman, Y. J. Chen *et al.*, "2 MB array-level demonstration of STT-MRAM process and performance towards L4 cache applications," *Proceedings of the IEDM*, pp. 2.4.1-2.4.4, 2019.

[5] G. Hu, J. J. Nowak, M. G. Gottwald, S. L. Brown, B. Doris *et al.*, "Spin-Transfer Torque MRAM with Reliable 2 ns Writing for Last Level Cache Applications," *Proceedings of the IEDM*, pp. 2.6.1-2.6.4, 2019.

[6] W. J. Gallagher, E. Chien, T. W. Chiang, J. C. Huang, M. C. Shih *et al.*, "22nm STT-MRAM for reflow and automotive uses with high yield, reliability, and magnetic immunity and with performance and shielding options," *Proceedings of the IEDM*, pp. 2.7.1-2.7.4, 2019.

[7] J. C. Slonczewski, "Current-driven excitation of magnetic multilayers," *Journal of Magnetization and Magnetic Materials*, vol. 159, pp. L1-L7, 1996.

[8] J. C. Slonczewski, "Currents, torques, and polarization factors in magnetic tunnel junctions," *Physical Review B*, vol. 71, p. 024411, 2005.

[9] C. Abert, M. Ruggeri, F. Bruckner, C. Vogler, G. Hrkac *et al.*, "A three-dimensional spin-diffusion model for micromagnetics," *Scientific Reports*, vol. 5, p. 14855, 2015.

[10] S. Lepadatu, "Unified treatment of spin torques using a coupled magnetisation dynamics and three-dimensional spin current solver," *Scientific Reports*, vol. 7, p. 12937, 2017.

[11] W. Skowronski, M.Czapkiewicz, S.Zietek, J.Checinski, M. Frankowski *et al.*, "Understanding stability diagram of perpendicular magnetic tunnel junctions," *Scientific Reports*, vol. 7, p. 10172, 2017.

[12] S. Bhatti, R. Sbiaa, A. Hirohata, H. Ohno, S. Fukami *et al.*, "Spintronics based random access memory: A review," *Materials Today*, vol. 20, pp. 530-548, 2017.

[13] S. Fiorentini, R. Orio, W. Goes, J. Ender, and V. Sverdlov, "Comprehensive comparison of switching models for perpendicular spin-transfer torque MRAM cells," *Proceedings of the SISPAD*, pp. 57-60, 2019.